Build orientation effect on Ti6Al4V thin-wall topography by electron beam powder bed fusion

Available online at www.sciencedirect.com

ScienceDirect

Procedia CIRP 108 (2022) 222–227

www.elsevier.com/locate/procedia

6th CIRP Conference on Surface Integrity

Build orientation effect on Ti6Al4V thin-wall topography by electron beam powder bed fusion

Giacomo Maculotti*, Gabriele Piscopo, Giovanni Marchiandi, Eleonora Atzeni, Alessandro Salmi, Luca Iuliano

Department of Management and Production Engineering, Politecnico di Torino, Corso Duca degli Abruzzi 24, 10129 Torino, Italy

* Corresponding author. *E-mail address:* giacomo.maculotti@polito.it

Abstract

Additive Manufacturing is a key enabling technology for Industry 4.0 and the Green Deal, allowing more efficient resources exploitation while providing innovative design to critical components. Electron Beam Powder Bed Fusion (EB-PBF) is an edge technology for many sectors, i.e. aerospace, medical, and automotive. The control of the surface finish by surface topography measurements is essential to engineer surface functional properties, whose specifications are application specific. This works investigates the effect of thin-wall orientation and surface inclination on the topography, described by areal field and feature parameters, to provide designers with a useful tool in the early stage of product development and tolerance specification and verification.

Keywords: Topography; Additive Manufacturing; Electron Beam Melting

1. Introduction

Additive Manufacturing (AM) technologies open up new perspectives in several sectors such as medical, automotive and aerospace [1,2]. According to Attaran [3], AM processes have superior attributes than conventional processes, and they are related to cost, speed, quality, innovation/transformation and environmental impact. Consequences are energy saving, material saving, recycling and a simpler supply chain that directly influence the sustainability of the manufacturing [4,5].

Among the metal AM processes, the Electron Beam Powder Bed Fusion process (EB-PBF) is an edge technology able to produce complex near net shape geometries of high melting point alloys [6,7]. Moreover, it is demonstrated that EB-PBF is the most sustainable metal AM process since it is characterized by the lowest environmental impact [8].

In the EB-PBF process, a rake is used to spread a thin layer of metal onto the building platform [1,9]. The layer of powder is firstly preheated and then the electron beam is focused and deflected in order to selectively melt the powder according to the part geometry [1,10]. The preheating phase ensures a lower temperature gradient along layers and hence prevent the formation of heat cracks and residual stresses [11]. In addition, the process is well suited for processing titanium alloys, that are characterized by a high reactivity with oxygen, since it is performed in a vacuum environment [7,11].

Despite the enormous advantages of the EB-PBF process, the produced parts typically suffer from poor surface quality. From present literature, it has been observed that the dimensional accuracy of EB-PBF samples is in the order of tenth of a millimetre [12] and the mean value of *Ra* commonly ranges between 20 µm and 50 µm [13,14]. In order to improve aesthetic, tribology or fatigue behaviour, subsequent finishing operations are necessary [6]. On the other hand, the rough surface of EBM samples could be an advantage in biomedical applications since it promotes osseointegration and biocompatibility [15-17], and has a positive influence on cell response [16]. According to the functionality of the surfaces

10.1016/j.procir.2022.03.039

and the desired quality, it is possible to tune the process and geometrical parameters [16].

Several works in the literature studied the surface properties of EBM parts. Wang *et al.* [18] studied the effect of two different scanning strategies that are the multispot and non-multispot contouring. Results showed that using non-multispot contouring the samples were characterized by a lower surface roughness. However, also the geometrical accuracy was lower, and this was attributed to the instability of the melt pool. Galati *et al.* [19] analysed the surface roughness of massive samples produced with different inclinations. As expected, the better surface roughness was obtained on upward surfaces, and the surface inclination strongly influenced the roughness value of upward surfaces. However, the roughness of downward surfaces was not significantly influenced by the surface orientation. Karlsson *et al.* [20] showed that samples produced with a fine powder particle size were characterized many unmelted particles and by a high peak to valley ratio. On the other hand, the layer thickness did not influence the surface quality. Safdar *et al.* [21] showed that the surface roughness of EBM samples increases with sample thickness and beam current, on the contrary, the surface roughness decreases with increasing offset focus and scan speed.

In the above-mentioned studies, the surface was characterized mainly by evaluating profile texture parameters or area field parameters, which give averaged data on the analysed profile or area such as *Ra* or *Sa*. However, the nature of AM surfaces cannot be fully captured by these parameters. In fact, AM surfaces are rich of features that represent the process signature, e.g. unmelted particles on the surface, topographical pores (dales) led by the propagation of inner defects, texture resulting by the scanning strategy, etc [22]. Accordingly, the literature has proposed a hybrid methodology combining texture parameters and feature-based characterization to thoroughly characterize AM native surface topographies [23]. Therefore, when investigating the relationship between the process parameters or the artefact shape and the surface characteristics of interest this larger and more complex set of parameters has to be considered, to properly guide the production of the desired surface texture without unwanted features. From the literature review emerges that most of the existing works analysed the surface quality, investigating the effect of process parameters and the effect of geometrical parameters of massive samples. However, the possibility to produce complex shapes, combined with a minimum support need, makes the use of EB-PBF process for the production of thin-walled structures very attractive. In fact, the use of thin-walled structure for the production of final component revolutionized the manufacturing sector, for thin walled structures allow reducing the weight the dimensions of the part and, consequently, saving money [1,24].

In this work, the effect of the inclination of thin-wall produced by EB-PBF on surface quality was investigated by means of surface topography analysis considering field and feature parameters, which is still unreported in the literature.

2. Methods and equipment

In the following paragraphs, the methods and the equipment used in the experimental investigation are described. Firstly, the geometry of the thin-wall test specimen is described, and the AM system used for its fabrication is illustrated. Then, the surface topography analysis method is presented, according to the most recent literature [23,25]. Last, the statistical analysis methodology to relate the thin-wall inclination to the resulting surface topography is presented.

2.1. Samples geometry and production

The test specimen geometry depicted in the Figure 1(a) was designed to evaluate the effect of the inclination on thin-wall surface quality. It includes four thin-walled planar features, each one characterized by an area of 30×20 mm² and a thickness of 2 mm, and a variable inclination. The inclination angle (α) with respect to the building platform and the orientation of the surface, depicted in Figure 1(b), are assumed as design variables. The inclination angle values are 30°, 50°, 70°, and 90°. The orientation is defined by the normal vector: the surface with the normal vector pointing towards the centre of the platform is called inner, the opposite outer.

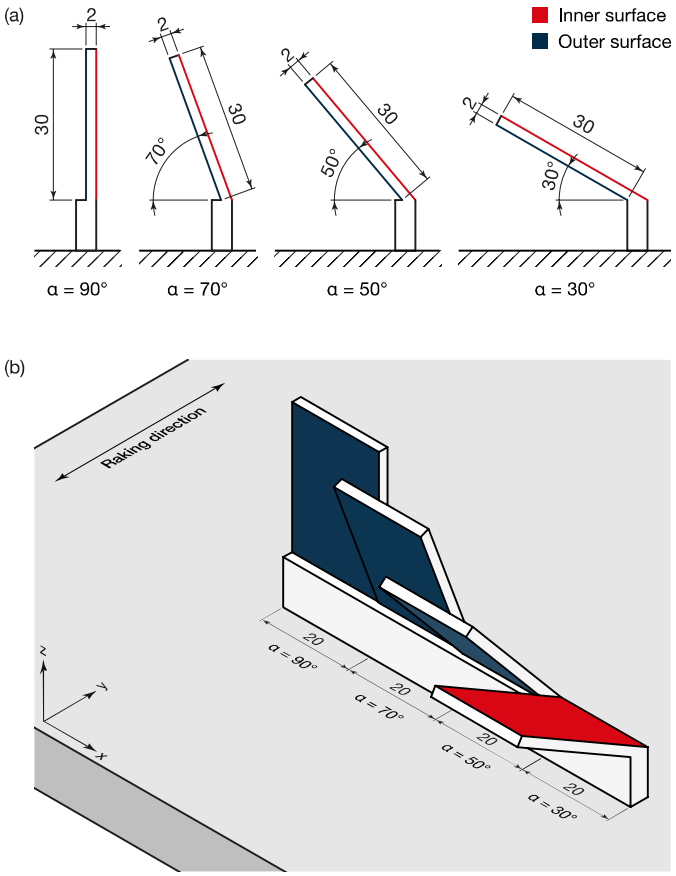

Figure 1. (a) Geometry of the test specimen and (b) inclination angle and orientation of the surfaces.

The test specimen was produced using an Arcam EBM A2X system adopting the standard process parameters (themes) and Ti6Al4V powder with a particles size ranging between 45 µm and 105 µm [19]. The layer thickness was set to 50 µm. For all the surfaces, with except to vertical ones, the inner surfaces coincide with upward surfaces and the outer surfaces correspond to downward surfaces. The thin-wall inclined by 30°, even if it includes a non-self-supporting surface, was produced without support structures to analyse the effect of this condition on the downward side.

2.2. Samples topographical characterization

Surface topography was measured by a state-of-the-art surface topography measuring instrument coherence scanning interferometer (CSI) Zygo NewView 9000 [26]. The instrument was set up to obtain a trade-off between measurement performances and measurement duration, according to literature best practices [27]. The instrument equipped a Mirau objective with numerical aperture 0.4 and a digital zoom 0.5x, resulting in a square pixel with lateral size of 0.87 µm. The field of view (FOV) is a square of 0.87×0.87 mm². Stitching of 4×4 FOV was performed to obtain a representative measured area of 2.856×2.856 mm². Measurements were performed with signal oversampling to relieve measurement disturbances and averaging 4 replicated measurements to diminish measurement noise [27]. One measurement per side of each thin-wall was performed. The measurement repeatability, the large measured area and the manufacturing process repeatability [6,23,25] allowed avoiding to perform replicated measurements. Measurements were characterized in state-of-the-art software Mountains Lab v8.0 according to the literature and the standard [23,25,28].

The first, measurement artefacts, i.e. non-measured points and spikes, were corrected [29]. Then, F-operator to suppress the nominal form of the surface, i.e. the plane, was removed by least-square fitting. Subsequently, the standard S-filter with nesting index of 10 µm to remove noise was applied. Last, the L-filter is applied to isolate the two topographical components, i.e. the waviness surface, at larger scales, and the scale limited SL-Surface, at smaller scales. The nesting index of the L-filter was chosen as the smooth-to-rough crossover (SRC) scale. The SRC is a spatial index that can be evaluated via multi-scale sensitive fractal analysis and that represent the spatial scale at which roughness can be first appreciated. This choice tailors the filtering to the actual spatial frequency content of the surface, thus avoiding the possible erroneous removal of relevant spatial components [30]. Both S- and L-Filter were chosen as Robust Gaussian filters to manage disturbances and end-effect [31]. The literature requires to characterize both the waviness surface and the SL-Surface. Table 1 summarizes the surface topography parameters and the evaluation surfaces.

Table 1. Considered surface topography parameter in the study and measurement units adopted in the result section.

Evaluation surface	Parameter	Unit
SF-Surface	SRC	µm
Waviness	S_a	µm
	S_q	µm
	S_{dq}	-
SL-Surface	V_p	mm³
	$A_{\%g}$	%
	V_p	mm³
	$A_{\%p}$	%
Feature-removed or *actual* SL-Surface	S_a	µm
	S_q	µm
	S_{dq}	-
	S_{sk}	-
	S_{ku}	-

The waviness surface is characterized by the area field parameters: *Sa*, *Sq*, *Sdq*. The SL-Surface is characterized by area feature parameters and area field parameters. The considered area feature parameters are the volume of protruding features, i.e. globules, and of topographical pores V_g and V_p, respectively, and the relative area over which those feature insist, i.e. $A_{\%g}$ and $A_{\%p}$. Identification of the topographical features is necessary to compute those parameters. Features are identified by watershed segmentation with pruning set at three times the *Sq* [23]. Once topographical features are identified, segmentation can be performed is isolate the *actual* SL-Surface, which can now be correctly characterized by area field parameters: *Sa*, *Sq*, *Sdq*, *Ssk* and *Sku*, without the contribution of a possible bias due to the presence of topographical feature [23,25].

2.3. Statistical analysis

This work investigates the effect of two factors on the surface topography of thin-wall structures: the build inclination of the surface itself (30°, 50°, 70°, and 90°) and the surface orientation (inner, outer). Excluding the vertical thin-wall, inner surfaces have a positive normal vector, and are upward oriented, whereas outer surfaces face the building platform.

The effect of these two factors can be investigated by means of a conventional ANoVA [32]. Because the surface orientation is a categorical factor and only presents two levels, and no replications have been considered, due to the high manufacturing and measurement reproducibility, the standard deviation within the orientation factor cannot be computed. Therefore, first a 1-way ANoVA is performed to test the statistical significance of the surface orientation. ANoVA is performed at the conventional confidence level of 95%. Then, linear least-square regression of the surface topography as a function of the inclination is performed. In the case the orientation results statistically significant, separated correlation empirical fitting functions are drawn for the two orientations between the topographic parameters and the thin-wall inclination. The statistics are performed in Minitab 17.

3. Results and discussion

The test specimen was successfully produced without evident defects and Figure 2 shows it. Measurement with CSI were performed, and Figure 3 shows the results of the topography measurements in pseudo-colour maps.

Surface topography characterization was performed according to Section 2.2, and related results are shown in Table 2, Table 3 and Table 4, respectively for area field parameters of waviness surface, feature parameters of SL-Surface and field parameters of the *actual* SF-Surface. It is worth remarking here that the obtained values refer to surfaces inherently rougher that the best performance that can be yielded by the EB-PBF process. In fact, due to their non-zero inclination, staircase effect and gravity induce natural rougher surfaces. Figure 4 shows the scatter plot of the considered surface topography parameters, which graphically supports the results obtained by means of ANoVA. ANoVA results are summarized in Table 5 which reports per each parameter if the considered factors introduce a systematic effect, i.e. if it is statistically significant at a confidence level of 95%.

Figure 2. Manufactured specimen fabricated by Arcam EBM A2X using Ti6Al4V powder and a layer thickness of 50 µm.

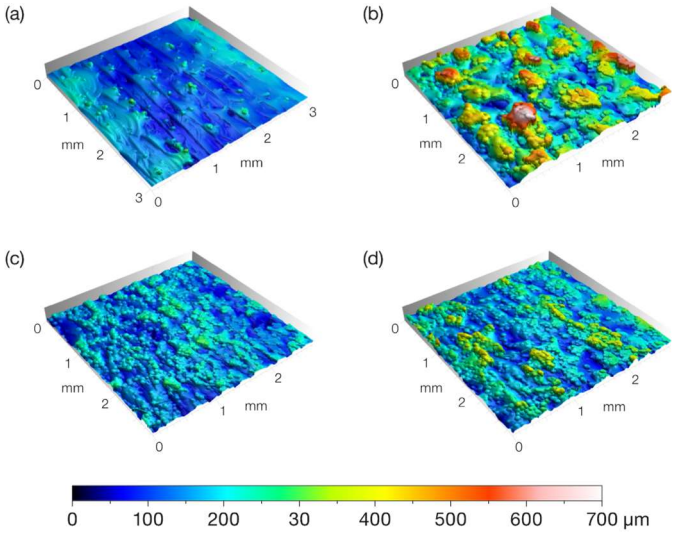

Figure 3. 3D pseudo-colour maps of the measured surface topography after application of S-Filter and F-Operator: (a) 30° inner, (b) 30° outer, (c) 90° inner, and (d) 90° outer.

Table 2. Area field parameter results for waviness surface and SRC related to the primary surface (after the removal of noise and form).

Orientation	α	SRC	S_a	S_q	S_{dq}
Inner	30°	231.9	18.83	23.62	0.22
	50°	194.9	20.87	26.75	0.33
	70°	209.9	28.05	34.80	0.44
	90°	163.9	30.78	39.04	0.54
Outer	30°	322.6	24.91	30.52	0.24
	50°	297.1	30.83	39.57	0.40
	70°	220.0	32.40	42.16	0.43
	90°	240.8	40.44	50.33	0.52

Table 3. Area feature parameter results for SL-Surface.

Orientation	α	$V_g \cdot 10^{-2}$	$A_{\%g}$	$V_p \cdot 10^{-2}$	$A_{\%p}$
Inner	30°	2.25	12.07	0.76	6.83
	50°	5.96	19.93	0.77	5.33
	70°	4.86	18.84	1.26	7.98
	90°	1.14	5.88	1.88	11.37
Outer	30°	9.86	15.34	4.35	11.49
	50°	9.78	18.23	1.89	8.46
	70°	1.16	5.42	0.72	4.50
	90°	3.51	8.58	1.60	6.67

Table 4. Area field parameter results for the *actual* SL-Surface.

Orientation	α	S_a	S_q	S_{dq}	S_{sk}	S_{ku}
Inner	30°	3.79	4.8	0.54	–0.41	2.98
	50°	4.01	5.1	0.85	–0.23	2.98
	70°	8.20	10.2	1.66	0.16	2.44
	90°	9.23	11.5	1.76	0.22	2.58
Outer	30°	10.03	11.8	2.35	–0.38	2.08
	50°	12.27	14.9	1.99	–0.06	2.29
	70°	11.78	15.1	1.78	–0.62	3.15
	90°	14.88	18.2	2.39	0.03	2.37

As it can be noticed, with a risk of error by 5%, the volume of globules and pores and the *Sku* of the *actual* SL-Surface are the only parameters that are not influenced by neither the surface orientation nor the thin-wall inclination. However, from Figure 4, it is possible to observe that on outer surfaces, a clear difference can be highlighted for both $A_{\%g}$ and V_g, when the inclination angle became higher than 50°. In particular, as the inclination angle increases, smaller globules acting on a smaller area are identified. However, the great data dispersion of the volume of globules leads the ANoVA to reject the hypothesis of significative impact of the orientation on the globules volume. This high dispersion also hinders the regression to infer a significantly robust empirical fitting functions between the globules volume and the orientation.

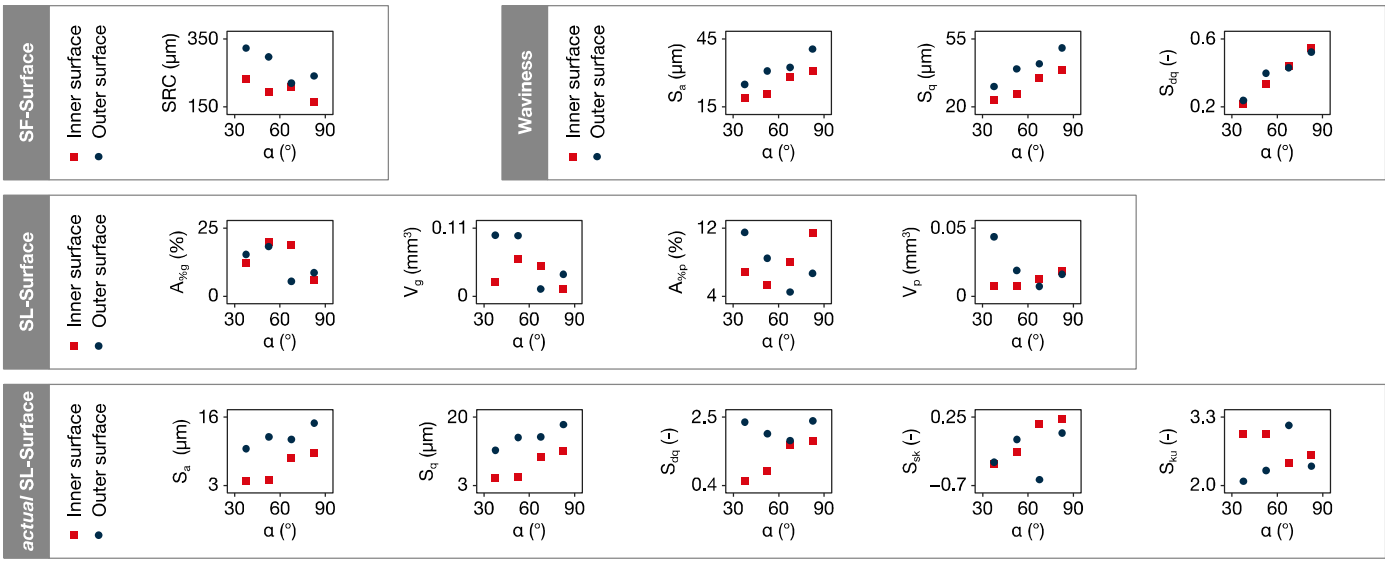

Figure 4. Scatter plot of the topographical parameters versus the thin-wall inclination angle for inner and outer surfaces.

As far as other topographical parameters are concerned, the orientation introduces a systematic component in all parameters but for the waviness surface *Sdq*, the SL-Surface feature parameters and its *Ssk*. Accordingly, the orientation does not affect the spatial variability and the steepness of the topography, which is well represented by *Sdq*, at large length scales; conversely these are significantly affected at small scales, i.e. for the SL-Surface. The inclination significantly affects all the considered surface topography parameters.

Table 5. Statistical analysis results. Surface orientation effect *p*-value investigated via ANoVA (if smaller than 0.05 indicates that the considered factor is statistically significant with a risk of error of 5%). Thin-wall inclination effect on parameter linear regression function and R^2.

Evaluation surface	Parameter	Orientation *p*-value	Empirical fitting function	R^2
SF-Surface	SRC	0.04	Inner: 256.8 – 0.95·α	0.73
			Outer: 366.9 – 1.61·α	0.76
Waviness	S_a	0.01	Inner: 11.72 + 0.22·α	0.95
			Outer: 17.72 + 0.24·α	0.94
	S_q	< 0.01	Inner: 14.76 + 0.27·α	0.97
			Outer: 22.04 + 0.31·α	0.96
	S_{dq}	0.52	0.095 + 0.005·α	0.96
SL-Surface	V_g	0.35	-	-
	$A_{\%g}$	0.62	$0.68·\alpha – 0.0067·\alpha^2$	0.92
	V_p	0.28	-	-
	$A_{\%p}$	0.96	$0.67·\alpha – 0.016·\alpha^2 + 1.03·10^{-4}·\alpha^3$	0.94
Feature-removed or *actual* SL-Surface	S_a	0.01	Inner: 0.105·α	0.99
			Outer: 8.02 + 0.07·α	0.82
	S_q	< 0.01	Inner: 0.131·α	0.99
			Outer: 9.21 + 0.97·α	0.92
	S_{dq}	0.03	Inner: 0.020·α	0.99
			Outer: $0.07·\alpha – 5.4·10^{-3}·\alpha^2$	0.95
	S_{sk}	0.40	–0.62 + 0.009·α	0.82
	S_{ku}	0.35	-	-

As far as other topographical parameters are concerned, the orientation introduces a systematic component in all parameters but for the waviness surface *Sdq*, the SL-Surface feature parameters and its *Ssk*. Accordingly, the orientation does not affect the spatial variability and the steepness of the topography, which is well represented by *Sdq*, at large length scales; conversely these are significantly affected at small scales, i.e. for the SL-Surface. The inclination significantly affects all the considered surface topography parameters.

The *Sa* value of actual inner and outer surfaces ranges between 3.79 µm and 9.23 µm and between 10.03 µm and 14.88 µm, respectively. This result agrees with the literature that shows that better surface morphology is obtained on upward surfaces [19,25]. This behaviour can be attributed to the different thermal phenomena acting on upward and downward surfaces. In fact, on upward surfaces, the heat is transferred through a solid material, instead on downward surface the heat is transferred through a powder bed. The heat dissipation is lower in the latter case and consequently, the higher temperatures cause an increased number of agglomerated particles that contribute to a higher roughness value on outer surfaces. All in all, in both cases the *Sa* value increases as the inclination angle increases. This means that on upward surfaces the staircase effect dictates the behaviour [19], instead on downward surfaces the heat dissipation and melted infiltrated material control the surface morphology [33].

Results are valid within the narrow process window of optimized parameters [19], which, though, ensure best trade-off between building time and part quality, e.g., full density, minimum residual stresses.

4. Conclusion

This work investigated the effect of surface orientation and inclination on the surface topography of thin-wall structures produced by EB-PBF. In optimized process conditions, state-of-the-art surface topography characterization relying both on conventional field parameters and less commonly adopted feature parameters is exploited to describe the surface topography. Thin-wall topography resulted to be affected by both the considered factors, i.e. the surface orientation and the wall inclination. The volume of topographical features is not affected, but their areal extension is.

Graphical investigation suggests that the presence of globules on outer surfaces seems to be influenced by the inclination angle. In particular, the volume and the extension area of globules sharply increased if the inclination angle was lower that 50°. It was found that two distinct phenomena govern the topography of the thin-wall surfaces. In particular, the topography of downward surfaces is mainly dependent on melted infiltrated material, but on upward surfaces the topography is dictated by the staircase effect.

Preliminary empirical fitting functions correlating the surface finish and the inclination of the thin-wall surface are drawn, whose robustness and representativeness can be augmented by future investigations. Future work will rely on these preliminary results to extend the investigation to tackle multi-scale geometrical characterization, include effect on mechanical properties and include in the analysis more geometrical design solutions.

Acknowledgements

This work has been partially supported by “Ministero dell’Istruzione, dell’Università e della Ricerca” Award “TESUN-83486178370409 finanziamento dipartimenti di eccellenza CAP. 1694 TIT. 232 ART. 6” and by resources provided by the Integrated Additive Manufacturing Interdepartmental Center (IAM@PoliTo) at the Politecnico di Torino, Turin, Italy.

References

[1] Gibson I, Rosen D, Stucker B. Additive Manufacturing Technologies, 2015.
[2] Piscopo G, Salmi A, Atzeni E. On the quality of unsupported overhangs produced by laser powder bed fusion. Int J Manuf Res. 2019;14:198-216.
[3] Attaran M. The rise of 3-D printing: The advantages of additive manufacturing over traditional manufacturing. Bus Horiz. 2017;60:677-88.
[4] Ahn DG. Direct Metal Additive Manufacturing Processes and Their Sustainable Applications for Green Technology: A Review. Int J Pr Eng Man-Gt. 2016;3:381-95.
[5] Ford S, Despeisse M. Additive manufacturing and sustainability: an exploratory study of the advantages and challenges. Journal of Cleaner Production. 2016;137:1573-87.
[6] Atzeni E, Rubino G, Salmi A, Trovalusci F. Abrasive fluidized bed finishing to improve the fatigue behaviour of Ti6Al4V parts fabricated by electron beam melting. Int J Adv Manuf Technol. 2020;110:557-67.
[7] Galati M, Iuliano L. A literature review of powder-based electron beam melting focusing on numerical simulations. Addit Manuf. 2018;19:1-20.
[8] Min W, Yang S, Zhang Y, Zhao YF. A Comparative Study of Metal Additive Manufacturing Processes for Elevated Sustainability. Volume 4: 24th Design for Manufacturing and the Life Cycle Conference; 13th International Conference on Micro- and Nanosystems2019.
[9] Galati M. Electron beam melting process. Addit Manuf, 2021. p. 277-301.
[10] Kumar S. Electron Beam Powder Bed Fusion. Cham: Springer International Publishing, 2020.
[11] Murr LE, Gaytan SM, Ramirez DA, Martinez E, Hernandez J, Amato KN, Shindo PW, Medina FR, Wicker RB. Metal Fabrication by Additive Manufacturing Using Laser and Electron Beam Melting Technologies. J Mater Sci Technol. 2012;28:1-14.
[12] Borrelli R, Franchitti S, Pirozzi C, Carrino L, Nele L, Polini W, Sorrentino L, Corrado A. Ti6Al4V Parts Produced by Electron Beam Melting: Analysis of Dimensional Accuracy and Surface Roughness. J Adv Manuf Syst. 2020;19:107-30.
[13] Galati M, Rizza G, Defanti S, Denti L. Surface roughness prediction model for Electron Beam Melting (EBM) processing Ti6Al4V. Precis Eng. 2021;69:19-28.
[14] Klingvall Ek R, Rännar L-E, Bäckstöm M, Carlsson P. The effect of EBM process parameters upon surface roughness. Rapid Prototyp J. 2016;22:495-503.
[15] Ruppert DS, Harrysson OLA, Marcellin-Little DJ, Abumoussa S, Dahners LE, Weinhold PS. Osseointegration of Coarse and Fine Textured Implants Manufactured by Electron Beam Melting and Direct Metal Laser Sintering. 3D Print Addit Manuf. 2017;4:91-7.
[16] Deligianni D. Effect of surface roughness of the titanium alloy Ti–6Al–4V on human bone marrow cell response and on protein adsorption. Biomaterials. 2001;22:1241-51.
[17] Fan H, Fu J, Li X, Pei Y, Li X, Pei G, Guo Z. Implantation of customized 3-D printed titanium prosthesis in limb salvage surgery: a case series and review of the literature. World Journal of Surgical Oncology. 2015;13.
[18] Wang P, Sin W, Nai M, Wei J. Effects of Processing Parameters on Surface Roughness of Additive Manufactured Ti-6Al-4V via Electron Beam Melting. Materials. 2017;10.
[19] Galati M, Minetola P, Rizza G. Surface Roughness Characterisation and Analysis of the Electron Beam Melting (EBM) Process. Materials. 2019;12.
[20] Karlsson J, Snis A, Engqvist H, Lausmaa J. Characterization and comparison of materials produced by Electron Beam Melting (EBM) of two different Ti–6Al–4V powder fractions. J Mater Process Technol. 2013;213:2109-18.
[21] Safdar A, He HZ, Wei LY, Snis A, Chavez de Paz LE. Effect of process parameters settings and thickness on surface roughness of EBM produced Ti‐6Al‐4V. Rapid Prototyp J. 2012;18:401-8.
[22] Senin N, Thompson A, Leach R. Feature-based characterisation of signature topography in laser powder bed fusion of metals. Meas Sci Technol. 2018;29.
[23] Lou S, Jiang X, Sun W, Zeng W, Pagani L, Scott PJ. Characterisation methods for powder bed fusion processed surface topography. Precis Eng. 2019;57:1-15.
[24] Gibson I, Rosen D, Stucker B. Design for Additive Manufacturing. Additive Manufacturing Technologies, 2015. p. 399-435.
[25] Newton L, Senin N, Chatzivagiannis E, Smith B, Leach R. Feature-based characterisation of Ti6Al4V electron beam powder bed fusion surfaces fabricated at different surface orientations. Addit Manuf. 2020;35.
[26] Thompson A, Senin N, Giusca C, Leach R. Topography of selectively laser melted surfaces: A comparison of different measurement methods. CIRP Annals. 2017;66:543-6.
[27] Gomez C, Su R, Thompson A, DiSciacca J, Lawes S, Leach R. Optimization of surface measurement for metal additive manufacturing using coherence scanning interferometry. Opt Eng. 2017;56.
[28] ISO 25178-2:2012 Geometrical product specifications (GPS) — Surface texture: Areal — Part 2: Terms, definitions and surface texture parameters. ISO, Genève.
[29] Maculotti G, Genta G, Quagliotti D, Galetto M, Hansen HN. Gaussian process regression ‐ based detection and correction of disturbances in surface topography measurements. Qual Reliab Eng Int. 2021.
[30] Brown CA, Johnsen WA, Butland RM, Bryan J. Scale-Sensitive Fractal Analysis of Turned Surfaces. CIRP Annals. 1996;45:515-8.
[31] Maculotti G, Feng X, Su R, Galetto M, Leach R. Residual flatness and scale calibration for a point autofocus surface topography measuring instrument. Meas Sci Technol. 2019;30.
[32] Montgomery DC, Runger GC, Hubele NF. Engineering statistics: John Wiley & Sons, 2009.
[33] Wu Z, Narra SP, Rollett A. Exploring the fabrication limits of thin-wall structures in a laser powder bed fusion process. Int J Adv Manuf Technol. 2020;110:191-207.